Sphingosine 1-phosphate activation of ERM contributes to vascular calcification[S]

Thomas G. Morris,* Samantha J. Borland,* Christopher J. Clarke,† Claire Wilson,* Yusuf A. Hannun,† Vasken Ohanian,* Ann E. Canfield,[1,*] and Jacqueline Ohanian[1,*]

Division of Cardiovascular Sciences,* School of Medical Sciences, Faculty of Biology, Medicine and Health, Manchester Academic Health Science Centre, University of Manchester, Manchester, United Kingdom; and Department of Medicine and Stony Brook Cancer Center,† Stony Brook University, Stony Brook, NY

Abstract **Vascular calcification is the deposition of mineral in the artery wall by vascular smooth muscle cells (VSMCs) in response to pathological stimuli. The process is similar to bone formation and is an independent risk factor for cardiovascular disease. Given that ceramide and sphingosine 1-phosphate (S1P) are involved in cardiovascular pathophysiology and biomineralization, their role in VSMC matrix mineralization was investigated. During phosphate-induced VSMC mineralization, endogenous S1P levels increased accompanied by increased sphingosine kinase (SK) activity and increased mRNA expression of SK1 and SK2. Consistent with this, mineralization was increased by exogenous S1P, but decreased by C2-ceramide. Mechanistically, exogenous S1P stimulated ezrin-radixin-moesin (ERM) phosphorylation in VSMCs and ERM phosphorylation was increased concomitantly with endogenous S1P during mineralization. Moreover, inhibition of acid sphingomyelinase and ceramidase with desipramine prevented increased S1P levels, ERM activation, and mineralization. Finally, pharmacological inhibition of ERM phosphorylation with NSC663894 decreased mineralization induced by phosphate and exogenous S1P. Although further studies will be needed to verify these findings in vivo, this study defines a novel role for the SK-S1P-ERM pathways in phosphate-induced VSMC matrix mineralization and shows that blocking these pathways with pharmacological inhibitors reduces mineralization. These results may inform new therapeutic approaches to inhibit or delay vascular calcification.**—Morris, T. G., S. J. Borland, C. J. Clarke, C. Wilson, Y. A. Hannun, V. Ohanian, A. E. Canfield, and J. Ohanian. **Sphingosine 1-phosphate activation of ERM contributes to vascular calcification.** ***J. Lipid Res.*** **2018.** 59: **69–78.**

Supplementary key words arteries • acid sphingomyelinase • biomineralization • cardiovascular disease • ceramides • ezrin • signal transduction • sphingosine kinase • smooth muscle cells • vascular biology • ezrin-radixin-moesin

Vascular calcification, the deposition of bone-like material in the media and/or intima of arteries, is an independent risk factor for cardiovascular disease (1). Vascular calcification is associated with aging and also occurs in response to injury and ionic and metabolic imbalance (2). There is now compelling evidence that vascular calcification is an active regulated process in which vascular smooth muscle cells (VSMCs) play an essential role. In response to pathological stimuli, such as inflammatory cytokines or mineral imbalance, VSMCs undergo osteogenic differentiation and apoptosis, releasing vesicles that initiate the deposition of a mineralized matrix (3, 4). Despite considerable research into the mechanisms and cellular processes that underlie vascular calcification, there are still no effective therapies to prevent or reverse the condition (5). Therefore, further understanding of the mechanisms that contribute to development of this pathology is essential in order to identify potential therapeutic strategies and targets.

The sphingolipids, ceramide and sphingosine 1-phosphate (S1P), are important signaling molecules, regulating many cellular processes that determine cell fate (6). Within the cardiovascular system, ceramide and S1P are implicated in vascular and cardiac morphogenesis, maintenance of vascular tone, vascular permeability, inflammation, aging, and atherosclerosis (7–12). Additionally, evidence is emerging that sphingolipids are involved in vascular and valvular calcification. For instance, in VSMCs, in vitro ceramide mediates oxidized-LDL (ox-LDL)-induced matrix

This work was supported by British Heart Foundation Grant FS/11/81/29331 a British Heart Foundation 4 year PhD studentship award to the University of Manchester.

Manuscript received 7 August 2017 and in revised form 11 November 2017.

Published, JLR Papers in Press, November 22, 2017
DOI https://doi.org/10.1194/jlr.M079731

Abbreviations: aCDase, acid ceramidase; aSMase, acid SMase; CDase, ceramidase; ERM, ezrin-radixin-moesin; HMU-PC, 6-hexadecanoylamino-4-methylumbelliferyl-phosphorylcholine; L-SMase, lysosomal aSMase; NBD-C6-SM, (6-((*N*-(7-nitrobenz-2-oxa-1,3-diazol-4-yl)amino)hexanoyl)-C6-sphingomyelin; nSMase, neutral SMase; ox-LDL, oxidized-LDL; pERM, phospho-ezrin-radixin-moesin; PKCα, protein kinase Cα; PP1α, protein phosphatase 1α; qPCR, quantitative RT-PCR; SK, sphingosine kinase; S1P, sphingosine 1-phosphate; VSMC, vascular smooth muscle cell.

[1]To whom correspondence should be addressed.
e-mail: Jacqueline.Ohanian@manchester.ac.uk (J.O.);
Ann.Canfield@manchester.ac.uk (A.E.C.)

[S] The online version of this article (available at http://www.jlr.org) contains a supplement.

mineralization (13) and neutral SMase (nSMase), which produces ceramide from sphingomyelin and regulates matrix vesicle release and subsequent VSMC matrix mineralization (14). Furthermore, a role for S1P in osteogenic differentiation and mineralization of human aortic valve interstitial cells has been reported (15). However, the mechanisms by which sphingolipids regulate VSMC matrix mineralization are still not fully understood.

A major source of ceramide within cells is from the hydrolysis of sphingomyelin by SMases. The main classes of SMase are acid SMase (aSMase) and nSMase, which are expressed ubiquitously and are also implicated in cell signaling (16–18). There are two forms of aSMase, secretory aSMase and lysosomal aSMase (L-SMase), which are the products of a single gene, *SMPD1*, but undergo alternative posttranslational modifications (19). L-SMase is active in lysosomes and forms part of the lysosomal sphingolipid salvage pathway (17). To date, four mammalian nSMases have been identified: *SMPD2* (nSMase1), *SMPD3* (nSMase2), *SMPD4* (nSMase3), and *SMPD5* (mitochondria-associated nSMase) (20). nSMases act on sphingomyelin at the plasma membrane. Activation of nSMase or L-SMase therefore results in production of ceramide in different subcellular compartments with access to different effectors. However, ceramide may not accumulate following SMase activation because it can be hydrolyzed rapidly by ceramidases (CDases) to produce sphingosine, the precursor of S1P (21, 22). Whereas many metabolic routes can form ceramide, there is only one source of S1P, the phosphorylation of sphingosine by sphingosine kinases (SKs) (SK1 and SK2, encoded by the genes *SPHK1* and *SPHK2*, respectively). Accordingly, alterations in the activity of enzymes within this pathway may lead to accumulation of ceramide and/or S1P within the cell. Indeed, lysomotropic inhibitors, such as desipramine, which induce proteolysis of L-SMase (23, 24) and acid CDase (aCDase) (25, 26), increase ceramide, and limit S1P production due to depletion of sphingosine (25).

Ceramide and S1P have emerged as important regulators of the ezrin-radixin-moesin (ERM) family of proteins. ERM proteins are activated by phosphorylation (27). In MCF7 breast cancer cells, S1P increases ERM phosphorylation (28); conversely, ceramide induces ERM dephosphorylation (6). In VSMCs, ERM proteins are implicated in proliferation, migration, and adhesion (29, 30). Although there have been no reports of ERM involvement in VSMC mineralization, several observations also link them to this process. For instance, ERM proteins are activated by Rho kinase and protein kinase Cα (PKCα) (27, 31) and both of these kinases have been implicated in VSMC mineralization (32–34). Ezrin also regulates Akt activity (35) and phosphate balance (36), both of which regulate VSMC mineralization (37–39). Finally, ERM proteins promote osteogenic differentiation of mesenchymal stem cells (40). Together these studies demonstrate that ERM proteins are activated by kinases that regulate mineralization and that they interact with proteins, which potentially regulate pathways that mediate vascular calcification.

Therefore, this study tests the hypothesis that VSMC mineralization is regulated by sphingolipids and investigates the role of ERM proteins in this process. Accordingly, we demonstrate for the first time that ceramide inhibits VSMC mineralization, whereas SIP is stimulatory. We also demonstrate that elevated-phosphate induces SK activity and increases SIP production, which stimulates matrix mineralization via activation of ERM signaling in VSMCs.

MATERIALS AND METHODS

Materials

Reagents were analytical grade and were obtained from Sigma-Aldrich (United Kingdom) unless otherwise stated. Desipramine was purchased from Sigma, NSC663894 from Merck Millipore, and C2-ceramide and S1P from Enzo Life Sciences. Anti-rabbit phospho-ezrin (Thr567)/radixin (Thr564)/moesin (Thr558) (#3149), anti-ezrin (#3145), anti-radixin (#2636), and anti-moesin (#3146) were from Cell Signaling Technology; anti-mouse β-actin (A1978) was from Sigma; and the HRP-conjugated secondary antibodies (#711-035-152 and #715-545-150) were from Jackson Immunoresearch.

Cell culture

VSMCs were isolated from bovine aortic explants and cultured in high glucose DMEM containing 10% (v/v) FBS, 100 U/ml penicillin, 0.1 mg/ml streptomycin, 1 mM sodium pyruvate, 2 mM L-glutamine, and 1× nonessential amino acids (10% FBS-DMEM). For experiments, VSMCs were seeded at 2×10^4 cells/cm^2 and maintained in 10% FBS-DMEM until 95% confluence (termed day 0). At this point, VSMCs were induced to mineralize by the addition of 3 or 5 mM β-glycerophosphate to 10% FBS-DMEM (osteogenic medium) (41). Control VSMCs were cultured in 10% FBS-DMEM alone (control medium). Medium was changed every 48 h up to 16 days. Two batches of VSMCs isolated from different animals were used in these studies. Cells were used between passage 8 and passage 11.

Cell treatments

For mineralization experiments in the presence of inhibitors [desipramine (1 and 10 μM); NSC668394 (1 and 10 μM)] or lipids [C2-ceramide (10 μM); S1P (0.01–10 μM)], cells were treated continuously from day 0. Where appropriate, an equivalent volume of vehicle was used as a control for each compound: deionized water (desipramine), DMSO (C2 ceramide, NSC668394). Medium, containing fresh inhibitors or lipids, was changed every 48 h for up to 16 days.

Quantification of mineralization

Alizarin red (40 mM, pH 4.1) was used to stain and visualize calcium-rich deposits (37). The extent of mineralization was quantified by dye elution (42). The stages of matrix mineralization in control cells incubated in osteogenic medium were based on absorbance values at 405 nm as follows: early mineralization 0.09–0.25, mid mineralization 0.25–1.25, and late mineralization 1.25–2.5 (arbitrary units).

Preparation of RNA and real-time quantitative RT-PCR analysis

Total RNA was isolated from VSMCs using the RNAeasy mini kit (Qiagen); 1 μg RNA was used to produce cDNA using TaqMan reverse transcription reagents (Applied Biosystems) in

an Eppendorf MasterCycler (Eppendorf). Quantitative RT-PCR (qPCR) using SYBR green was performed for *SMPD1* (aSMase), *SPHK1* (SK1), and *SPHK2* (SK2) in a standard reaction mix of 12 μl containing 50 ng of cDNA, 0.83 μM forward and reverse primers, and 1× SYBR green PCR master mix (Applied Biosystems) using a CFX96 real-time system (Bio-Rad). Primer sequences are shown in supplemental Table S1. Samples were heated to 95°C for 10 min, followed by 40 cycles of: 95°C for 15 s, 60°C for 1 min, and 72°C for 15 s. Amplification of a single PCR product was confirmed by melt-curve analysis and PCR products were sequenced using a 3730 DNA analyzer (Applied Biosystems) to confirm that the correct target had been amplified. qPCR using TaqMan gene expression assays (Applied Biosystems) was performed for *SMPD2* (nSMase1; GenBank™ accession number NM_001075383.2), *SMPD3* (nSMase2; GenBank™ accession number NM_001192363.1), and *SMPD4* (nSMase3; GenBank™ accession number NM_001205602.1). The standard reaction mix was 20 μl containing 82.5 ng of cDNA, 0.9 μM forward and reverse primers, 0.25 μM of the reporter probe, and 1× TaqMan gene expression master mix (Applied Biosystems) using the same real-time system as above. Samples were heated to 95°C for 10 min, followed by 40 cycles of 95°C for 15 s and 60°C for 1 min. For both assays, reactions were performed in duplicate and averaged to give one data point. Values were normalized to housekeeping genes (PPIA and RPL12) and results were calculated using the comparative Ct (threshold cycle) method (43).

Immunoblotting

Cells were washed with PBS and lysed in RIPA buffer [50 mM Tris (pH 7.4), 150 mM NaCl, 25 nM sodium deoxycholate, 1% Triton X-100, 3.5 mM sodium dodecyl sulfate, 5% glycerol, 1 mM dithiothreitol, 50 μM sodium orthovanadate, 200 μM sodium pyrophosphate, and protease inhibitors (Complete Mini-tab; Roche)] at 4°C for 20 min before centrifugation at 12,000 *g* for 15 min at 4°C. The protein concentration of the lysate was estimated by Bradford assay (Bio-Rad) and adjusted to 1.2 mg/ml before addition of 5× Laemmli sample buffer, giving a final protein concentration of 1 mg/ml. Equivalent amounts of protein (20–50 μg) were subjected to SDS-PAGE, transferred to nitrocellulose membrane, blocked in TBS/0.1% Tween containing 5% fish skin gelatin, and probed with anti-rabbit phospho-ezrin (Thr567)/radixin (Thr564)/moesin (Thr558), ezrin, radixin, or moesin (1:1,000 in TBS/0.1% Tween containing 0.1% fish skin gelatin, overnight at 4°C) and anti-mouse β-actin (1:10,000 in TBS/0.1% Tween containing 0.1% fish skin gelatin, 30 min at room temperature) as loading control, followed by the appropriate HRP-conjugated secondary antibody (1:10,000 in TBS/0.1% Tween containing 0.1% fish skin gelatin). Signals were developed with chemiluminescence, imaged using a Chemidoc (Bio-Rad), and band intensities quantified using Chemidoc software (Bio-Rad).

SMase and SK activity assays

Cells were washed with PBS and lysed in Tris-TX-100 buffer [50 mM Tris (pH 7.4), 5 mM EDTA, 0.2% Triton X-100, protease inhibitors (Complete mini-tab, Roche), 1 mM sodium orthovanadate, and 200 μM sodium pyrophosphate] at 4°C for 20 min before centrifugation at 12,000 *g* for 15 min at 4°C. The protein concentration of the supernatant was determined by Bradford assay (Bio-Rad) and adjusted to 1 mg/ml.

nSMase activity was measured in cell lysates using (6-((*N*-(7-nitrobenz-2-oxa-1,3-diazol-4-yl)amino)hexanoyl)-C6-sphingomyelin (NBD-C6-SM) as described previously (10). Briefly, cell lysate (50 μg protein) was added to 100 μl of reaction mixture containing 100 mM Tris (pH 7.4), 10 mM $MgCl_2$, 0.2% Triton X-100, 10 mM dithiothreitol, 100 μM NBD-C6-SM, and 100 μM phosphatidylserine. Following a 30 min incubation at 37°C, reactions were terminated by the addition of 1 ml chloroform:methanol (2:1 v:v) and 200 μl dH_2O for phase separation. The upper aqueous phase was discarded and the lower organic phase dried under O_2-free N_2 gas and resuspended in 15 μl chloroform:methanol (2:1 v:v). Samples and NBD-C6-ceramide standard were spotted onto heat-activated silica gel 60 thin-layer chromatography plates (Merck) and developed in chloroform/methanol/10% NH_4OH (7/3/0.5 v/v/v). The plates were air-dried and the fluorescent lipid detected using an Alpha-Innotech imager. NBD-C6-ceramide was identified by the co-chromatographed standard and quantified by densitometry using AlphaEaseFC software. Lysosomal-SMase activity was measured using 6-hexadecanoylamino-4-methylumbelliferyl-phosphorylcholine (HMU-PC) (44). Briefly, cell lysate (25 μg protein) was added to 55 μl of reaction mixture containing 750 mM sodium acetate (pH 5.2), 0.3% Triton X-100, 3 mM EDTA, and 1.5 mM HMU-PC. After 1 h at 37°C, 500 μl of stop buffer [0.5 M sodium bicarbonate (pH 10.7), 0.25% Triton X-100) were added and fluorescence measured in a 300 μl aliquot using excitation 404 nm and emission 460 nm filters [FLx800 microplate reader (BioTek)]. The levels of liberated HMU were quantified using an HMU standard curve.

SK activity was measured using a commercial SK activity assay kit (Echelon Biosciences, Salt Lake City, UT) according to the manufacturer's instructions. In brief, cell lysate (5 μg protein) was incubated in reaction buffer containing 100 μM sphingosine and 10 μM ATP for 20 min at room temperature. The reaction was stopped by addition of 40 μl luminescence-conjugated ATP detector, and kinase activity was measured using an Orion L microplate luminometer (Titertek-Berthold).

Measurement of sphingolipids

For lipid analysis by mass spectrometry, VSMCs were washed with PBS, lysed in RIPA buffer for 20 min at 4°C, and protein concentration determined by Bradford assay (Bio-Rad). Total cell lysate containing 0.5 mg protein was analyzed for ceramide, dihydroceramide, and sphingoid bases by tandem liquid chromatography/mass spectrometry (45). Lipid levels were normalized to cellular total protein. Lipid analysis was carried out at the Lipidomics Core Facility, Stony Brook University Medical Center, Stony Brook, NY.

Data analysis

The data are shown as the mean ± SEM, as indicated in the appropriate figure legends. Statistical analyses were performed using a Student's *t*-test or a one-way or two-way ANOVA followed by multiple comparison post hoc test, as indicated in the figure legends. Results were deemed significant when $P < 0.05$. All statistics were calculated using GraphPad Prism 7.

RESULTS

Inhibition of the sphingolipid salvage pathway reduces VSMC matrix mineralization

To investigate the role of the sphingolipid salvage pathway (**Fig. 1A**) in matrix mineralization, VSMCs were cultured in osteogenic medium or osteogenic medium plus desipramine, a dual L-SMase and aCDase inhibitor (25, 26), for up to 14 days. Control cells were incubated in control medium. Deposition of a mineralized matrix was assessed and quantified by alizarin red staining at three time points corresponding to early, mid, and late mineralization

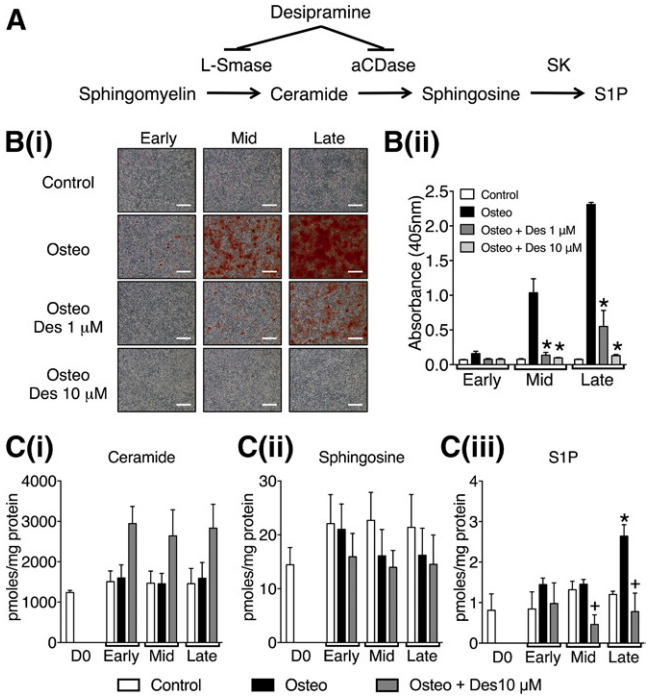

Fig. 1. The effect of desipramine on VSMC matrix mineralization and sphingolipid levels. A: Diagram of the lysosomal sphingolipid salvage pathway showing points in the pathway inhibited by desipramine. B: VSMCs were cultured in control, osteogenic (Osteo), or osteogenic with 1 or 10 μM desipramine (Des) medium. Matrix mineralization was detected and quantified by alizarin red staining. B(i): Photomicrographs representative of early, mid, and late stages of mineralization shown by positive alizarin staining (red); scale bar = 500 μm. B(ii): Quantification of matrix mineralization by elution of alizarin red. Data are mean ± SEM from three independent experiments, $*P < 0.05$ for osteogenic versus osteogenic plus desipramine. C: Mass spectroscopy analysis of ceramide [C(i)], sphingosine [C(ii)], and S1P [C(iii)] from VSMCs at day 0 (D0) and the early, mid, and late stages of mineralization. Data are mean ± SEM from three independent experiments. $+P < 0.05$ for osteogenic versus osteogenic plus desipramine; $*P < 0.05$ for control versus osteogenic, by two-way ANOVA with Dunnett's multiple comparisons post test.

(Fig. 1B). Incubation with desipramine (1 or 10 μM) in the presence of osteogenic medium significantly inhibited matrix mineralization compared with cells incubated with osteogenic medium and vehicle (Fig. 1B).

In order to determine whether desipramine might inhibit VSMC matrix mineralization through effects on the sphingolipid salvage pathway, we measured the levels of ceramide, sphingosine, and S1P at early, mid, and late mineralization with and without desipramine (10 μM). When cells were incubated in osteogenic medium, a marked increase in S1P levels was detected at the late stage of mineralization, this increase was abolished by co-incubation with desipramine (Fig. 1C). Ceramide levels were similar in VSMCs cultured in osteogenic medium compared with controls at the same time points (Fig. 1C). However, in the presence of 10 μM desipramine, there was a trend to increased ceramide throughout the mineralization time course (Fig. 1C), consistent with inhibition of the lysosomal sphingolipid salvage pathway (Fig. 1A). Further analysis of the species of ceramide in VSMCs demonstrated that culture in osteogenic medium did not affect the levels of any individual species throughout the time course of mineralization compared with controls (**Fig. 2**). However, incubation with desipramine significantly increased the levels of several individual ceramide species, C14, C22, C24:1, C24, C26:1, and C26 ceramides (Fig. 2). Together these data suggest that S1P levels are increased during mineralization of VSMCs as a consequence of increased ceramide flux through the lysosomal sphingolipid pathway, and that interfering with this pathway using desipramine limits the biosynthesis of S1P and inhibits mineralization.

Exogenous ceramide inhibits and S1P stimulates VSMC matrix mineralization

To explore whether ceramide and/or S1P regulate the deposition of a mineralized matrix by VSMCs, the effect of exogenous ceramide and S1P on VSMC matrix mineralization was studied. Incubation of VSMCs with the cell-permeable C2-ceramide (10 μM) in osteogenic medium decreased matrix mineralization compared with controls incubated in osteogenic medium plus vehicle (**Fig. 3A**). In contrast, exogenous S1P (10 μM) increased matrix mineralization (Fig. 3B). Prolonged treatment with C2-ceramide or S1P had no effect on VSMCs cultured in control medium (supplemental Fig. S1A, B). These data demonstrate that S1P and C2-ceramide have opposing effects on VSMC matrix mineralization.

The mRNA expression of SK1 and SK2 and SK activity increases during VSMC matrix mineralization

Ceramide and S1P are generated by SMase-mediated hydrolysis of sphingomyelin and sphingosine phosphorylation by SKs, respectively (Fig. 1A). Accordingly we next determined whether changes in SK or SMase activity and/or expression correlated with the increase in S1P production during deposition of a mineralized matrix by VSMCs. Total RNA was isolated from confluent day 0 VSMCs and VSMCs cultured in control or osteogenic medium at early, mid, and late mineralization and the mRNA expression levels of SKs [*SPHK1* (SK1) and *SPHK2* (SK2)] and sphingomyelinases [*SMPD1* (aSMase), *SMPD2* (nSMase1), *SMPD3* (nSMase2), and *SMPD4* (nSMase3)] determined by qPCR. To investigate whether any changes observed in mRNA levels of sphingomyelinases and SKs lead to functional effects, enzyme activities of SK, L-SMase, and N-SMase were also measured at the same time points.

SPHK1 (SK1) and *SPHK2* (SK2) mRNA levels were increased at mid mineralization and *SPHK2* (SK2) remained elevated at late mineralization in VSMCs in osteogenic medium (Fig. 4A). Concomitant with elevated mRNA levels, SK activity was also increased at late-mineralization. The increased expression and activity of the SKs occurred at the same time point at which high levels of S1P were measured [Fig. 1C(iii)]. There was no change in *SPHK1* (SK1) and *SPHK2* (SK2) mRNA levels in VSMCs in control medium at any time point (**Fig. 4A**). Similarly, SK activity remained unchanged throughout prolonged culture in control medium (Fig. 4A). To confirm that the changes in SK mRNAs were associated with deposition of a mineralized matrix

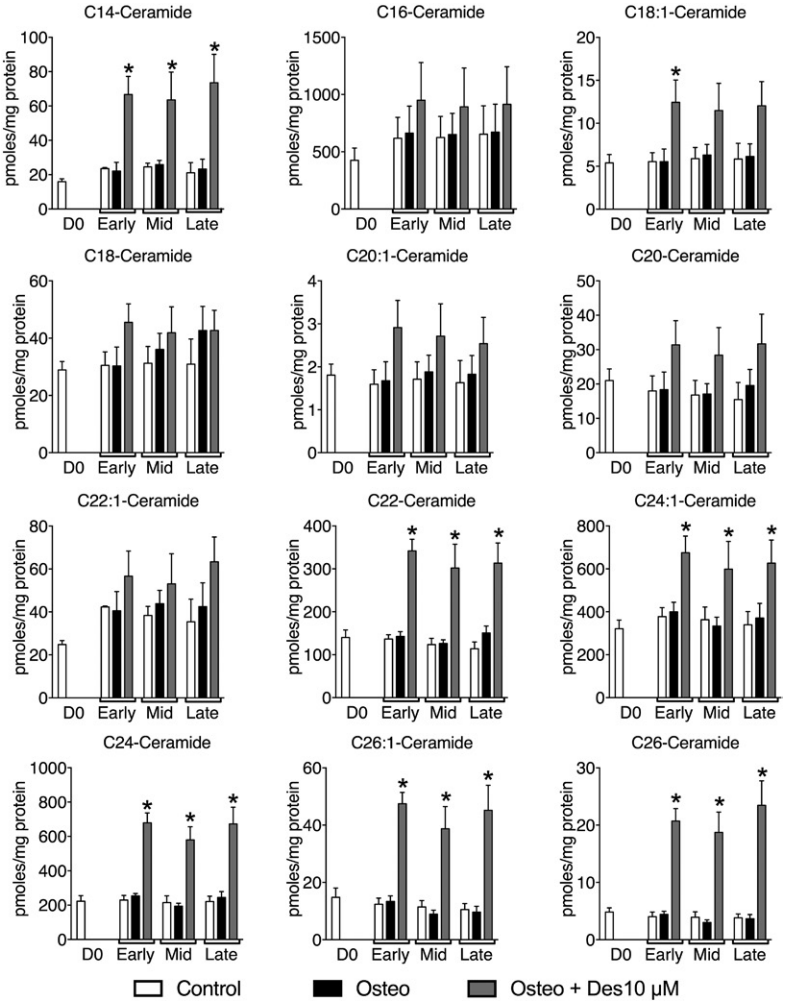

Fig. 2. The effect of desipramine on individual ceramide species during VSMC matrix mineralization. VSMCs were cultured in control, osteogenic, or osteogenic with 10 μM desipramine medium. Individual ceramide species were analyzed using mass spectroscopy from VSMCs at day 0 (D0) and early, mid, and late stages of matrix mineralization. The data are mean ± SEM from three independent experiments. *$P < 0.05$ for osteogenic versus osteogenic plus 10 μM desipramine by two-way ANOVA with Dunnett's multiple comparisons post test.

and not a consequence of prolonged exposure to high phosphate, a separate population of VSMCs that did not deposit a mineralized matrix in response to osteogenic medium was studied. There was no change in *SPHK1* (SK1) or *SPHK2* (SK2) mRNA up to 12 days of culture in either control or osteogenic medium in these cells (supplemental Fig. S2).

Next, we investigated whether changes in SMase mRNA expression and/or activity changed throughout the mineralization time course. *SMPD1* (aSMase) mRNA levels did not change in VSMCs cultured in either control or osteogenic medium (Fig. 4B). The mRNA levels of *SMPD2* (nSMase1) did not change during culture in control medium, but increased in VSMCs in osteogenic medium at late mineralization (Fig. 4B). In contrast, *SMPD4* (nSMase3) mRNA levels increased over the mineralization time course, but there was no difference between VSMCs in control and osteogenic medium (Fig. 4B). *SMPD3* (nSMase2) mRNA was not detected in the VSMCs at any of the time points tested (not shown), even though these primers could detect *SMPD3* mRNA in aortic endothelial cells (supplemental Fig. S3).

To explore whether changes in *SMPD1*, *-2*, and *-4* mRNA expression led to changes in enzyme activity, L-SMase and nSMase activity was measured. Both L-SMase and nSMase activity increased between day 0 and the early mineralization time point and remained elevated throughout the time course in both control and osteogenic medium. Only at late mineralization was there a difference between control and osteogenic medium when L-SMase (Fig. 4C) and nSMase (Fig. 4C) activity decreased in the mineralizing cells.

Taken together, we show that during the deposition of a mineralized matrix there is increased SK1 and SK2 mRNA expression, SK activity, and increased S1P in VSMCs, which is accompanied by a decrease in both L-SMase and nSMase activity. These data are consistent with the hypothesis that endogenous sphingolipids are implicated in the regulation of matrix mineralization.

Mechanisms involved in S1P-induced matrix mineralization of VSMCs

To explore the mechanisms involved in sphingolipid regulation of matrix mineralization, we investigated the adaptor proteins, ezrin, radixin, and moesin, which have been identified as downstream effectors of ceramide and S1P signaling (6, 28). Ceramide and S1P reciprocally regulate ERM activity by inducing dephosphorylation and phosphorylation, respectively, at the activation sites, Thr567-ezrin, Thr564-radixin, and Thr558-moesin, (27). Immunoblot analysis

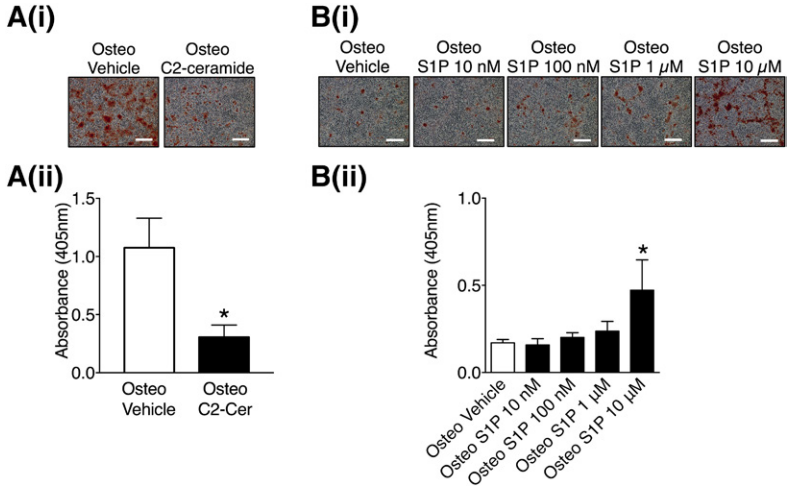

Fig. 3. The effect of C2-ceramide and S1P on VSMC matrix mineralization. A: VSMCs were cultured in osteogenic (Osteo) or osteogenic with 10 μM C2-ceramide medium. At mid mineralization, the cells were stained with alizarin red. Representative photomicrographs showing mineralization (red), scale bar = 500 μm [A(i)] and quantification of matrix mineralization by elution of alizarin red [A(ii)]. Data are mean ± SEM from six independent experiments. $*P < 0.05$ osteogenic versus osteogenic plus C2-ceramide by paired *t*-test. B: VSMCs were cultured in osteogenic medium with the indicated concentrations of S1P. At early mineralization, the cells were stained with alizarin red. Representative photomicrographs showing mineralization (red), scale bar = 500 μm [B(i)] and quantification of matrix mineralization by elution of alizarin red [B(ii)]. Data are mean ± SEM from three independent experiments. $*P < 0.05$ osteogenic versus osteogenic plus S1P by one-way ANOVA with Tukey's multiple comparisons post test.

identified ezrin and moesin in VSMC lysates; radixin was not detected (**Fig. 5A**). The lack of detection of radixin in our VSMCs may reflect poor antibody cross-reactivity with bovine radixin because radixin is expressed in rat aortic VSMCs (30). Next, we investigated whether ERM phosphorylation was altered during VSMC matrix mineralization. Protein lysates were prepared from VSMCs cultured in control, osteogenic, or osteogenic plus desipramine medium at early, mid, and late mineralization. For all time points, lysates were prepared from cells 48 h post medium change. A phospho-ezrin-radixin-moesin (pERM) antibody that recognizes phosphorylation of all three proteins at the activating threonine detected a marked increase in pERM levels in mineralized VSMCs compared with controls (Fig. 5B). Indeed, a doublet was detected by the pERM antibody, suggesting that both ezrin (81 kDa) and moesin (78 kDa) were activated. Interestingly, the increase in ERM phosphorylation in VSMCs in osteogenic medium compared with control correlated with the time point of increased S1P (Fig. 1). Furthermore, desipramine, which prevents S1P production and matrix mineralization (Fig. 1), prevented the increase in ERM phosphorylation in VSMCs in osteogenic medium (Fig. 5B). Whether ceramide or S1P activate ERM proteins in VSMCs has not been reported, so it was investigated here. Immunoblot analysis demonstrated that short-term (5 and 10 min) stimulation of VSMCs with 10 μM C2-ceramide did not alter pERM levels (Fig. 5C). In contrast, 10 μM S1P increased pERM levels at both 5 and 10 min (Fig. 5C), demonstrating a potential for S1P to activate ERM proteins in VSMCs.

These data suggest that S1P-induced activation of ERM is important for regulating VSMC matrix mineralization.

S1P-induced ezrin activation is necessary for VSMC matrix mineralization

The ezrin inhibitor, NSC668394, which inhibits ezrin Thr-567 phosphorylation (46), was used to investigate whether ezrin activity is important for matrix mineralization. Initially, to confirm that NSC668394 inhibited S1P activation of ezrin, VSMCs were incubated with 1 or 10 μM NSC668394 for 16 h before stimulation with 10 μM S1P for 10 min. Preincubation with NSC668394 (1 μM) did not prevent S1P-induced ezrin phosphorylation (**Fig. 6A**). However, at the higher concentration of 10 μM, NSC668394 did inhibit the increase in phospho-ezrin in response to S1P (Fig. 6A). Accordingly, the effect of 10 μM NSC668394 on VSMC matrix mineralization was studied. These experiments demonstrated that 10 μM of NSC668394 markedly inhibited mineralization (Fig. 6B). Prolonged treatment with 10 μM of NSC668394 had no effect on VSMCs cultured in control medium (supplemental Fig. S1C). Finally, rescue experiments were performed where VSMCs were coincubated in osteogenic medium with 10 μM of NSC668394 and 10 μM of S1P. Under these conditions, S1P was unable to overcome the inhibitory effect of NSC668394, whereas S1P alone promoted mineralization, as reported above (Fig. 6B).

These data demonstrate that inhibition of S1P-induced phosphorylation of ezrin is important for VSMC matrix mineralization, identifying a novel pathway for regulation of vascular calcification.

DISCUSSION

Our results establish several novel findings regarding the regulation of VSMC matrix mineralization by sphingolipids and the mechanisms by which they exert their effects. First, our inhibition studies using desipramine show that VSMC matrix mineralization is regulated, at least in part, through sphingolipids generated via the lysosomal sphingolipid pathway. Second, lipid analysis demonstrates that S1P increases during VSMC matrix mineralization, and using qPCR and activity assays, we show that increased mRNA expression and activation of SKs directly correlate with S1P production, implicating this pathway as a key regulator of matrix mineralization. Third, we show that activation of ERM proteins is required for VSMC matrix mineralization and that ERM activation requires elevated S1P levels. Furthermore, in the presence of ezrin inhibition, S1P is no

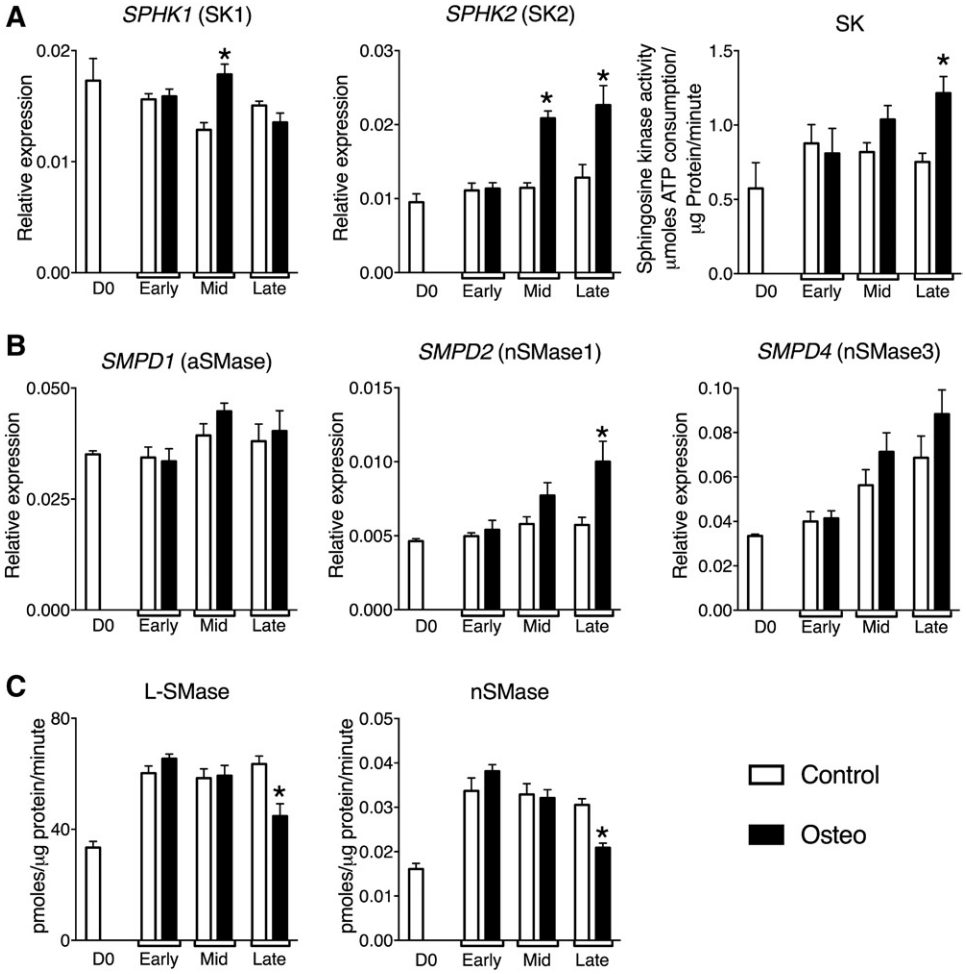

Fig. 4. The mRNA expression profile and activity of SKs and SMases during VSMC matrix mineralization. VSMCs were cultured in control or osteogenic (Osteo) medium. At day 0 (D0), early, mid, and late mineralization cell lysates were prepared for activity assays or total RNA was extracted for quantification of target genes by qPCR. *SPHK1* and *SPHK2* expression, SK activity (A); *SMPD1*, *SMPD2*, and *SMPD4* expression (B); and L-SMase and nSMase activity (C). mRNA levels are shown relative to the housekeeping genes, PP1A and RPL12, as detailed in the Materials and Methods. The data are mean ± SEM from eight independent experiments. $*P < 0.05$ control versus osteogenic by two-way ANOVA with Dunnett's multiple comparisons post test.

longer able to stimulate matrix mineralization, identifying ezrin as a downstream mediator of S1P-induced VSMC mineralization. Finally, we show that, in contrast to S1P, ceramide inhibits VSMC matrix mineralization. Taken together, these results demonstrate that therapeutic manipulation of VSMC sphingolipid metabolism by inhibition of the lysosomal sphingolipid salvage pathway inhibits VSMC matrix mineralization.

We detected an increase in cellular SIP in VSMCs cultured in osteogenic medium when mineralization was widespread. Within the cell, S1P is formed by SK-mediated phosphorylation of sphingosine. During matrix mineralization, the mRNA expression of SK1 and SK2 and SK activity increased in VSMCs concomitant with an increase in intracellular S1P, although only increased SK2 mRNA expression directly correlated with SK activity and elevated S1P levels, implicating this isoform in VSMC matrix mineralization. Use of desipramine to inhibit S1P production prevented VSMC matrix mineralization, confirming the importance of sphingolipid flux through this pathway. However, we cannot rule out that decreased degradation of S1P [by either S1P lyase or S1P phosphate phosphohydrolases (21)] may also contribute to the increase in intracellular S1P levels at late mineralization. Also, we showed that exogenous S1P increases phosphate-induced VSMC matrix mineralization. However, 10 μM S1P was required to consistently increase the rate of phosphate-induced VSMC mineralization, which is approximately 10-fold higher than human plasma concentrations (47, 48); although our studies were conducted in the presence of 10% FBS, which would bind S1P and lower the effective concentration. Additionally, we tested lower S1P concentrations and observed a trend to increased mineralization with 1 μM S1P, indicating that the threshold for increasing mineralization is between 1 and 10 μM S1P in vitro in the presence of 10% FBS. A requirement for supraphysiological concentrations of exogenous S1P to increase phosphate-induced VSMC mineralization may reflect uptake into the cells and activation of intracellular pathways (49). We did not measure cellular S1P levels following addition of exogenous S1P; therefore, a direct

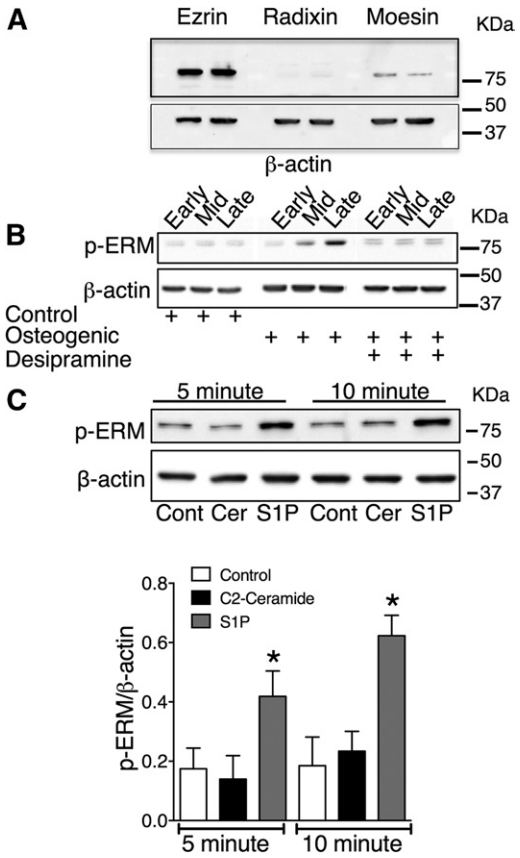

Fig. 5. S1P-dependent activation of ERM during VSMC matrix mineralization. A: Cell lysates were prepared from confluent VSMCs cultured in control medium for immunoblot analysis for ezrin, radixin, and moesin. β-Actin was used as a loading control. An immunoblot with duplicate samples is shown. B: VSMCs were cultured in control osteogenic or osteogenic with desipramine (10 μM) medium, and cell lysates prepared for immunoblot analysis with pERM at early, mid, and late matrix mineralization. β-Actin was used as a loading control. The immunoblot is representative of three independent experiments. C: VSMCs were stimulated with 10 μM C2-ceramide (Cer) or 10 μM S1P for 5 or 10 min and cell lysates prepared for immunoblot analysis for pERM. β-Actin was used as a loading control (Cont). Representative immunoblot and densitometric data of pERM corrected for loading are shown. The data are mean ± SEM from three independent experiments. $*P < 0.05$ for control versus 10 μM S1P by one-way ANOVA with Tukey's multiple comparisons post test.

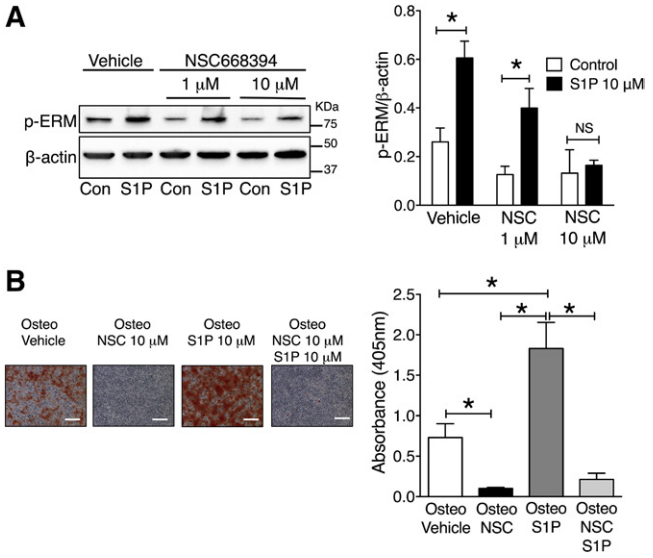

Fig. 6. Inhibition of S1P-dependent activation of ERM prevents VSMC matrix mineralization. A: VSMCs were incubated with vehicle (0.1% DMSO), 1 μM NSC668394 (NSC), or 10 μM NSC668394 for 16 h before stimulation with 10 μM S1P for 10 min, and cell lysates prepared for immunoblot analysis with pERM. β-Actin was used as a loading control (Con). Representative immunoblot and densitometric data of pERM corrected for loading are shown. The data are mean ± SEM from three independent experiments. $*P < 0.05$ for control versus 10 μM S1P by two-way ANOVA with Dunnett's multiple comparisons post test. B: VSMCs were cultured in osteogenic (Osteo) medium, osteo plus NSC668394 (NSC) (10 μM), osteo plus S1P (10 μM), or osteo plus NSC668394 (10 μM) plus S1P (10 μM). At the mid-mineralization time point, cells were stained with alizarin red. Representative photomicrographs showing mineralization (red), scale bar = 500 μm and quantification of matrix mineralization by elution of alizarin red. Data are mean ± SEM from six independent experiments. $*P < 0.05$ by one-way ANOVA with Tukey's multiple comparisons post test.

comparison between the increase in endogenous S1P observed in cells in osteogenic medium and the effects of exogenous S1P was not possible. However, our study does demonstrate that S1P is a major regulator of biomineralization by VSMCs, and suggests that under osteogenic conditions, such as high phosphate in chronic kidney disease, VSMCs may be a source of S1P, which could further predispose to vascular calcification.

In addition to inhibiting S1P production, desipramine treatment of VSMCs in osteogenic medium increased ceramide levels throughout early, mid, and late mineralization. Desipramine induces downregulation of aSMase and aCDase within lysosomes, which can lead to ceramide accumulation within the lysosome (23–26). Therefore, treatment of VSMCs in osteogenic medium with desipramine shifted the cellular balance between ceramide and S1P, which may contribute to the inhibition of mineralization by desipramine. These data, therefore, prompted us to investigate the effects of ceramide on VSMC matrix mineralization. Cell-permeable C2-ceramide decreased VSMC mineralization in osteogenic medium, suggesting that increased ceramide in the presence of desipramine could be involved in the prevention of mineralization observed with this inhibitor. However, there is evidence that water-soluble C2-ceramide may not directly mimic the effects of hydrophobic long-chain endogenous ceramides (50). Accordingly, further studies are required to substantiate the role of ceramide in vascular calcification. Indeed, an inhibitory role for ceramide is in direct contrast to a recent report in human femoral artery VSMCs where ceramide was identified as a mediator of ox-LDL-induced matrix mineralization (13). The reasons for these apparently opposing results are unclear. In the latter study (13), ox-LDL was shown to rapidly and transiently increase nSMase activity and ceramide levels in human femoral artery VSMCs and an inhibitor of nSMase2 prevented mineralization. Activation of nSMase will produce ceramide outside of the lysosomal compartment, giving the ceramide access to different effectors compared with generation of ceramide by L-SMase, which

remains trapped within the lysosomes. Kapustin et al. (14) have reported that, in human coronary artery VSMCs, nSMase2 inhibition prevents matrix vesicle release and reduces mineralization in response to osteogenic medium. However, although we could detect nSmase1 and nSmase3 expression in the VSMCs used in our study, we could not detect nSMase2. Therefore, differences in response to ceramide may reflect the different nSMases expressed. It is also noteworthy that neither of the studies in human VSMCs (13, 14) investigated whether endogenous ceramide levels changed during matrix mineralization; accordingly, stimulation of mineralization may have been due to conversion of ceramide to S1P.

A further novel finding of our study is that ERM phosphorylation is required for VSMC matrix mineralization. To our knowledge, this is the first report that ERM proteins are potential regulators of vascular calcification. Our demonstration that S1P stimulates ERM phosphorylation in VSMCs is in agreement with studies in HeLa and breast cancer cells (51, 52). Interestingly, in HeLa cells stimulated with epidermal growth factor, SK2-derived S1P induced ERM phosphorylation (51), which may also suggest that increased expression of SK2 during VSMC mineralization may be regulating ERM activity. It should be noted that the signaling data was obtained following short-term addition of S1P, whereas effects on mineralization were observed during treatment up to 16 days. However, a time course demonstrated that ERM phosphorylation increased at mid and late VSMC mineralization when increased cellular S1P was also detected. Furthermore, using NSC668394, a small molecule inhibitor of ezrin threonine-567 phosphorylation (46), we showed that ezrin activity is required for VSMC mineralization. Thus, NSC668394 blocked S1P-induced ERM phosphorylation and VSMC matrix mineralization. Additionally, S1P was unable to overcome the inhibition of matrix mineralization by NSC668394, demonstrating that ezrin acts downstream of S1P to regulate calcification. Similarly, desipramine, which prevented the S1P increase and VSMC mineralization, also prevented ERM phosphorylation, although it is also possible that, in the presence of desipramine, increased ceramide levels induced ERM dephosphorylation. Ceramide activates protein phosphatase 1α (PP1α) to dephosphorylate ERM (53). However, whether ceramide in the lysosomal compartment would have access to cytosolic PP1α is unclear. Certainly addition of cell permeable C2-ceramide to VSMCs did not reduce basal ERM phosphorylation, which might suggest that, during mineralization, increased S1P is the key regulator of this pathway.

In this study, we used small molecule inhibitors of lysosomal sphingolipid metabolism and ezrin activity, desipramine and NSC663894, respectively. We believe that our study is the first to show that inhibition of these pathways may be clinically relevant in vascular calcification. Although further work with in vivo models of vascular calcification is required to substantiate our in vitro findings, studies in cancer have demonstrated that lysosomotropic agents, such as desipramine, sensitize cancer cells to chemotherapeutic agents and ezrin inhibition prevents osteosarcoma metastasis (54, 55). Taken together, these findings and our study suggest that using small molecule inhibitors of these pathways may be of clinical relevance.

In summary, this study has demonstrated, in VSMCs, that inhibition of S1P formation prevents, whereas exogenous S1P stimulates, matrix mineralization induced by osteogenic medium. Moreover, we have identified ERM proteins as important downstream effectors of S1P-induced VSMC matrix mineralization in vitro. These novel findings add further evidence to the growing recognition of S1P as a regulator of vascular pathologies. Further work is now required to determine how ERM proteins regulate VSMC matrix mineralization and to explore the potential of desipramine as an inhibitor of vascular calcification in vivo.

REFERENCES

1. Rennenberg, R. J., A. G. Kessels, L. J. Schurgers, J. M. van Engelshoven, P. W. de Leeuw, and A. A. Kroon. 2009. Vascular calcifications as a marker of increased cardiovascular risk: a meta-analysis. *Vasc. Health Risk Manag.* **5:** 185–197.
2. Demer, L. L., and Y. Tintut. 2014. Inflammatory, metabolic, and genetic mechanisms of vascular calcification. *Arterioscler. Thromb. Vasc. Biol.* **34:** 715–723.
3. Sage, A. P., Y. Tintut, and L. L. Demer. 2010. Regulatory mechanisms in vascular calcification. *Nat. Rev. Cardiol.* **7:** 528–536.
4. Sallam, T., H. Cheng, L. L. Demer, and Y. Tintut. 2013. Regulatory circuits controlling vascular cell calcification. *Cell. Mol. Life Sci.* **70:** 3187–3197.
5. Boström, K. I. 2016. Where do we stand on vascular calcification? *Vascul. Pharmacol.* **84:** 8–14.
6. Zeidan, Y. H., R. W. Jenkins, and Y. A. Hannun. 2008. Remodeling of cellular cytoskeleton by the acid sphingomyelinase/ceramide pathway. *J. Cell Biol.* **181:** 335–350.
7. Alewijnse, A. E., and S. L. M. Peters. 2008. Sphingolipid signalling in the cardiovascular system: good, bad or both? *Eur. J. Pharmacol.* **585:** 292–302.
8. Chatterjee, S. 1998. Sphingolipids in atherosclerosis and vascular biology. *Arterioscler. Thromb. Vasc. Biol.* **18:** 1523–1533.
9. Hla, T., and A. J. Dannenberg. 2012. Sphingolipid signaling in metabolic disorders. *Cell Metab.* **16:** 420–434.
10. Ohanian, J., S. P. Forman, G. Katzenberg, and V. Ohanian. 2012. Endothelin-1 stimulates small artery VCAM-1 expression through p38MAPK-dependent neutral sphingomyelinase. *J. Vasc. Res.* **49:** 353–362.
11. Ohanian, J., A. Liao, S. P. Forman, and V. Ohanian. 2014. Age-related remodeling of small arteries is accompanied by increased sphingomyelinase activity and accumulation of long-chain ceramides. *Physiol. Rep.* **2:** e12015.
12. Smith, A. R., F. Visioli, B. Frei, and T. M. Hagen. 2006. Age-related changes in endothelial nitric oxide synthase phosphorylation and nitric oxide dependent vasodilation: evidence for a novel mechanism involving sphingomyelinase and ceramide-activated phosphatase 2A. *Aging Cell.* **5:** 391–400.
13. Liao, L., Q. Zhou, Y. Song, W. Wu, H. Yu, S. Wang, Y. Chen, M. Ye, and L. Lu. 2013. Ceramide mediates ox-LDL-induced human vascular smooth muscle cell calcification via p38 mitogen-activated protein Kinase Signaling. *PLoS One.* **8:** e82379.
14. Kapustin, A. N., M. L. L. Chatrou, I. Drozdov, Y. Zheng, S. M. Davidson, D. Soong, M. Furmanik, P. Sanchis, R. T. M. De Rosales, D. Alvarez-Hernandez, et al. 2015. Vascular smooth muscle cell calcification is mediated by regulated exosome secretion. *Circ. Res.* **116:** 1312–1323.
15. Fernández-Pisonero, I., J. López, E. Onecha, A. I. Dueñas, P. Maeso, M. S. Crespo, J. A. S. Román, and C. García-Rodríguez. 2014. Synergy between sphingosine 1-phosphate and lipopolysaccharide signaling promotes an inflammatory, angiogenic and osteogenic response in human aortic valve interstitial cells. *PLoS One.* **9:** e109081.
16. Wu, B. X., C. J. Clarke, and Y. A. Hannun. 2010. Mammalian neutral sphingomyelinases: regulation and roles in cell signaling responses. *Neuromolecular Med.* **12:** 320–330.

17. Jenkins, R. W., D. Canals, and Y. A. Hannun. 2009. Roles and regulation of secretory and lysosomal acid sphingomyelinase. *Cell. Signal.* **21:** 836–846.
18. Airola, M. V., and Y. A. Hannun. 2013. Sphingolipid metabolism and neutral sphingomyelinases. *Handb. Exp. Pharmacol.* **215:** 57–76.
19. Schissel, S. L., G. A. Keesler, E. H. Schuchman, K. J. Williams, and I. Tabas. 1998. The cellular trafficking and zinc dependence of secretory and lysosomal sphingomyelinase, two products of the acid sphingomyelinase gene. *J. Biol. Chem.* **273:** 18250–18259.
20. Clarke, C. J., B. X. Wu, and Y. A. Hannun. 2011. The neutral sphingomyelinase family: identifying biochemical connections. *Adv. Enzyme Regul.* **51:** 51–58.
21. Pyne, N. J., J. S. Long, S. C. Lee, C. Loveridge, L. Gillies, and S. Pyne. 2009. New aspects of sphingosine 1-phosphate signaling in mammalian cells. *Adv. Enzyme Regul.* **49:** 214–221.
22. Maceyka, M., K. B. Harikumar, S. Milstien, and S. Spiegel. 2012. Sphingosine-1-phosphate signaling and its role in disease. *Trends Cell Biol.* **22:** 50–60.
23. Hurwitz, R., K. Ferlinz, G. Vielhaber, H. Moczall, and K. Sandhoff. 1994. Processing of human acid sphingomyelinase in normal and I-cell fibroblasts. *J. Biol. Chem.* **269:** 5440–5445.
24. Kölzer, M., N. Werth, and K. Sandhoff. 2004. Interactions of acid sphingomyelinase and lipid bilayers in the presence of the tricyclic antidepressant desipramine. *FEBS Lett.* **559:** 96–98.
25. Zeidan, Y. H., B. J. Pettus, S. Elojeimy, T. Taha, L. M. Obeid, T. Kawamori, J. S. Norris, and Y. A. Hannun. 2006. Acid ceramidase but not acid sphingomyelinase is required for tumor necrosis factor-{alpha}-induced PGE2 production. *J. Biol. Chem.* **281:** 24695–24703.
26. Elojeimy, S., D. H. Holman, X. Liu, A. El-Zawahry, M. Villani, J. C. Cheng, A. Mahdy, Y. Zeidan, A. Bielwaska, Y. A. Hannun, et al. 2006. New insights on the use of desipramine as an inhibitor for acid ceramidase. *FEBS Lett.* **580:** 4751–4756.
27. Matsui, T., M. Maeda, Y. Doi, S. Yonemura, M. Amano, K. Kaibuchi, S. Tsukita, and S. Tsukita. 1998. Rho-kinase phosphorylates COOH-terminal threonines of ezrin/radixin/moesin (ERM) proteins and regulates their head-to-tail association. *J. Cell Biol.* **140:** 647–657.
28. Canals, D., R. W. Jenkins, P. Roddy, M. J. Hernández-Corbacho, L. M. Obeid, and Y. A. Hannun. 2010. Differential effects of ceramide and sphingosine 1-phosphate on ERM phosphorylation: probing sphingolipid signaling at the outer plasma membrane. *J. Biol. Chem.* **285:** 32476–32485.
29. Zhang, Y-X., J-T. Xu, X-C. You, C. Wang, K-W. Zhou, P. Li, P. Sun, L. Wang, and T-H. Wang. 2016. Inhibitory effects of hydrogen on proliferation and migration of vascular smooth muscle cells via down-regulation of mitogen/activated protein kinase and ezrin-radixin-moesin signaling pathways. *Chin. J. Physiol.* **59:** 46–55.
30. Baeyens, N., I. Latrache, X. Yerna, G. Noppe, S. Horman, and N. Morel. 2013. Redundant control of migration and adhesion by ERM proteins in vascular smooth muscle cells. *Biochem. Biophys. Res. Commun.* **441:** 579–585.
31. Ng, T., M. Parsons, W. E. Hughes, J. Monypenny, D. Zicha, A. Gautreau, M. Arpin, S. Gschmeissner, P. J. Verveer, P. I. Bastiaens, et al. 2001. Ezrin is a downstream effector of trafficking PKC-integrin complexes involved in the control of cell motility. *EMBO J.* **20:** 2723–2741.
32. Chen, N. X., X. Chen, K. D. O'Neill, S. J. Atkinson, and S. M. Moe. 2010. RhoA/Rho kinase (ROCK) alters fetuin-A uptake and regulates calcification in bovine vascular smooth muscle cells (BVSMC). *Am. J. Physiol. Renal Physiol.* **299:** F674–F680.
33. Lee, K., H. Kim, and D. Jeong. 2014. Protein kinase C regulates vascular calcification via cytoskeleton reorganization and osteogenic signaling. *Biochem. Biophys. Res. Commun.* **453:** 793–797.
34. Borland, S. J., T. G. Morris, S. C. Borland, M. R. Morgan, S. E. Francis, C. L. R. Merry, and A. E. Canfield. 2017. Regulation of vascular smooth muscle cell calcification by syndecan-4/FGF-2/PKCα signalling and cross-talk with TGFβ. *Cardiovasc. Res.* **113:** 1639–1652.
35. Wu, K. L., S. Khan, S. Lakhe-Reddy, G. Jarad, A. Mukherjee, C. A. Obejero-Paz, M. Konieczkowski, J. R. Sedor, and J. R. Schelling. 2004. The NHE1 Na+/H+ exchanger recruits ezrin/radixin/moesin proteins to regulate Akt-dependent cell survival. *J. Biol. Chem.* **279:** 26280–26286.
36. Mahon, M. J. 2008. Ezrin promotes functional expression and parathyroid hormone-mediated regulation of the sodium-phosphate cotransporter 2a in LLC-PK1 cells. *Am. J. Physiol. Renal Physiol.* **294:** F667–F675.
37. Collett, G. D. M., A. P. Sage, J. P. Kirton, M. Y. Alexander, A. P. Gilmore, and A. E. Canfield. 2007. Axl/phosphatidylinositol 3-kinase signaling inhibits mineral deposition by vascular smooth muscle cells. *Circ. Res.* **100:** 502–509.
38. Heath, J. M., Y. Sun, K. Yuan, W. E. Bradley, S. Litovsky, L. J. Dell'Italia, J. C. Chatham, H. Wu, and Y. Chen. 2014. Activation of AKT by O-linked N-acetylglucosamine induces vascular calcification in diabetes mellitus. *Circ. Res.* **114:** 1094–1102.
39. Shanahan, C. M., M. H. Crouthamel, A. Kapustin, and C. M. Giachelli. 2011. Arterial calcification in chronic kidney disease: key roles for calcium and phosphate. *Circ. Res.* **109:** 697–711.
40. Titushkin, I., and M. Cho. 2011. Altered osteogenic commitment of human mesenchymal stem cells by ERM protein-dependent modulation of cellular biomechanics. *J. Biomech.* **44:** 2692–2698.
41. Shioi, A., Y. Nishizawa, S. Jono, H. Koyama, M. Hosoi, and H. Morii. 1995. β-Glycerophosphate accelerates calcification in cultured bovine vascular smooth muscle cells. *Arterioscler. Thromb. Vasc. Biol.* **15:** 2003–2009.
42. Gregory, C. A., W. G. Gunn, A. Peister, and D. J. Prockop. 2004. An alizarin red-based assay of mineralization by adherent cells in culture: comparison with cetylpyridinium chloride extraction. *Anal. Biochem.* **329:** 77–84.
43. Schmittgen, T. D., and K. J. Livak. 2008. Analyzing real-time PCR data by the comparative C(T) method. *Nat. Protoc.* **3:** 1101–1108.
44. van Diggelen, O. P., Y. V. Voznyi, J. L. M. Keulemans, K. Schoonderwoerd, J. Ledvinova, E. Mengel, M. Zschiesche, R. Santer, and K. Harzer. 2005. A new fluorimetric enzyme assay for the diagnosis of Niemann-Pick A/B, with specificity of natural sphingomyelinase substrate. *J. Inherit. Metab. Dis.* **28:** 733–741.
45. Bielawski, J., J. S. Pierce, J. Snider, B. Rembiesa, Z. M. Szulc, and A. Bielawska. 2010. Sphingolipid analysis by high performance liquid chromatography-tandem mass spectrometry (HPLC-MS/MS). *Adv. Exp. Med. Biol.* **688:** 46–59.
46. Bulut, G., S-H. Hong, K. Chen, E. M. Beauchamp, S. Rahim, G. W. Kosturko, E. Glasgow, S. Dakshanamurthy, H-S. Lee, I. Daar, et al. 2012. Small molecule inhibitors of ezrin inhibit the invasive phenotype of osteosarcoma cells. *Oncogene.* **31:** 269–281.
47. Hammad, S. M., J. S. Pierce, F. Soodavar, K. J. Smith, M. M. Al Gadban, B. Rembiesa, R. L. Klein, Y. A. Hannun, J. Bielawski, and A. Bielawska. 2010. Blood sphingolipidomics in healthy humans: impact of sample collection methodology. *J. Lipid Res.* **51:** 3074–3087.
48. Hammad, S. M., M. M. Al Gadban, A. J. Semler, and R. L. Klein. 2012. Sphingosine 1-phosphate distribution in human plasma: associations with lipid profiles. *J. Lipids.* **2012:** 180705.
49. Van Brocklyn, J. R., M. J. Lee, R. Menzeleev, A. Olivera, L. Edsall, O. Cuvillier, D. M. Thomas, P. J. Coopman, S. Thangada, C. H. Liu, et al. 1998. Dual actions of sphingosine-1-phosphate: extracellular through the Gi-coupled receptor Edg-1 and intracellular to regulate proliferation and survival. *J. Cell Biol.* **142:** 229–240.
50. Wagenknecht, B., W. Roth, E. Gulbins, H. Wolburg, and M. Weller. 2001. C2-ceramide signaling in glioma cells: synergistic enhancement of CD95-mediated, caspase-dependent apoptosis. *Cell Death Differ.* **8:** 595–602.
51. Adada, M. M., D. Canals, N. Jeong, A. D. Kelkar, M. Hernandez-Corbacho, M. J. Pulkoski-Gross, J. C. Donaldson, Y. A. Hannun, and L. M. Obeid. 2015. Intracellular sphingosine kinase 2-derived sphingosine-1-phosphate mediates epidermal growth factor-induced ezrin-radixin-moesin phosphorylation and cancer cell invasion. *FASEB J.* **29:** 4654–4669.
52. Orr Gandy, K. A., M. Adada, D. Canals, B. Carroll, P. Roddy, Y. A. Hannun, and L. M. Obeid. 2013. Epidermal growth factor-induced cellular invasion requires sphingosine-1-phosphate/sphingosine-1-phosphate 2 receptor-mediated ezrin activation. *FASEB J.* **27:** 3155–3166.
53. Canals, D., P. Roddy, and Y. A. Hannun. 2012. Protein phosphatase 1 alpha mediates ceramide-induced ERM dephosphorylation: a novel mechanism independent of PIP2 and myosin/ERM phosphatase. *J. Biol. Chem.* **287:** 10145–10155.
54. Kuzu, O. F., M. Toprak, M. A. Noory, and G. P. Robertson. 2017. Effect of lysosomotropic molecules on cellular homeostasis. *Pharmacol. Res.* **117:** 177–184.
55. Ren, L., and C. Khanna. 2014. Role of ezrin in osteosarcoma metastasis. *Adv. Exp. Med. Biol.* **804:** 181–201.